

Cite this: *Chem. Sci.*, 2015, 6, 917

Tandem redox mediator/Ni(II) trihalide complex photocycle for hydrogen evolution from HCl†

Seung Jun Hwang,^a David C. Powers,^a Andrew G. Maher^{ab} and Daniel G. Nocera^{*a}

Photoactivation of M–X bonds is a challenge for photochemical HX splitting, particularly with first-row transition metal complexes because of short intrinsic excited state lifetimes. Herein, we report a tandem H₂ photocycle based on combination of a non-basic photoredox phosphine mediator and nickel metal catalyst. Synthetic studies and time-resolved photochemical studies have revealed that phosphines serve as photochemical H-atom donors to Ni(II) trihalide complexes to deliver a Ni(I) centre. The H₂ evolution catalytic cycle is closed by sequential disproportionation of Ni(I) to afford Ni(0) and Ni(II) and protolytic H₂ evolution from the Ni(0) intermediate. The results of these investigations suggest that H₂ photogeneration proceeds by two sequential catalytic cycles: a photoredox cycle catalyzed by phosphines and an H₂-evolution cycle catalyzed by Ni complexes to circumvent challenges of photochemistry with first-row transition metal complexes.

Received 4th August 2014
Accepted 7th October 2014

DOI: 10.1039/c4sc02357a

www.rsc.org/chemicalscience

Introduction

The photochemical splitting of hydrohalic acids (HX) into H₂ and X₂ is an approach to solar fuel synthesis¹ that stores a comparable amount of energy to water splitting. In addition to the similar energy densities implicit in HX and H₂O splitting chemistries, HX splitting mandates management of only two electrons and two protons, whereas H₂O splitting requires management of four protons and four electrons.^{2–5} Photocatalytic HX splitting requires accomplishing multielectron photochemical reactions to activate strong M–X bonds. Typically, photoreduction has been the limiting step in HX splitting photocatalysis and often X₂ elimination requires the use of chemical traps for evolved halogen equivalents.^{6–17} Attempts at promoting HX splitting with first-row transition metal complexes are attractive given that these metals are typically earth abundant, but have been largely unsuccessful. The challenge of using first-row metal complexes as HX splitting photocatalysts is that photochemical activation of Ni(I) or Ni(II) halides frequently does not lead to photoreduction reactions,^{18,19} likely due to the short excited state lifetimes of first-row transition metal complexes.^{20–22}

To overcome the short excited state lifetimes typical of first-row complexes, we have pursued a photoredox strategy for H₂ evolution from HCl in which the photochemistry and H₂ evolution roles are separated between a photoredox mediator and a hydrogen-evolution catalyst, respectively.²³ We were attracted to this strategy because it does not rely on molecular excited states of first-row metal complexes. In our first foray into photoredox catalysis for H₂ evolution, we employed bipyridines as photoredox mediators and Ni polypyridyl complexes as H₂ evolution catalysts. H-atom abstraction (HAA) by the excited state of the bipyridine afforded a pyridinyl radical, which engaged with a Ni(II) halide complex to generate a Ni(I) intermediate *via* halogen radical abstraction. The resulting Ni(I) complex underwent disproportionation to a Ni(II) complex and a Ni(0) species, which subsequently engaged in protolytic H₂ evolution. While these efforts demonstrated a synthetic cycle for H₂ evolution, H₂-evolution catalysis was not observed because the basic bipyridyl photoredox mediator was passivated in the presence of HCl.

To address the challenges of photoredox catalysis for H₂ evolution from HCl, we turned our attention to identifying a photoredox mediator that could function under acidic conditions. We now examine the role of phosphines as photoredox mediators under acidic conditions (pK_a in CH₃CN: PPh₃ = 7.64; pyridine = 12.53).²⁴ The photochemical homolysis of P–H bonds of 2° phosphines generates phosphinyl radicals that display sufficient lifetime (~160 μs) to participate in halogen-atom abstraction from a Ni(II) halide complex to furnish a reduced Ni intermediate that participates in an H₂ evolution cycle; the phosphine photoredox mediator is regenerated by HAA from solvent to close the photocycle.^{25–27} The H₂-evolution cycle may

^aDepartment of Chemistry and Chemical Biology, 12 Oxford Street, Cambridge, MA 02138-2902, USA. E-mail: dnocera@fas.harvard.edu

^bDepartment of Chemistry, Massachusetts Institute of Technology, 77 Massachusetts Avenue, Cambridge, MA 02139-4307, USA

† Electronic supplementary information (ESI) available: Experimental procedures and time-dependent photochemical data; transient absorption spectroscopy and electrochemical experimental details. CCDC 992218–992221. For ESI and crystallographic data in CIF or other electronic format see DOI: 10.1039/c4sc02357a



eventually be closed by thermally promoted protolytic H₂ evolution with HCl.

Experimental

Materials and methods

All reactions were carried out in an N₂-filled glovebox. Anhydrous solvents were obtained by filtration through drying columns.²⁸ NMR chemical shifts are reported in ppm with the residual solvent resonance as internal standard. UV-vis spectra were recorded at 293 K in quartz cuvettes on a Spectral Instruments 400 series diode array and were blanked against the appropriate solvent. PhICl₂²⁹ and Ni(PPh₃)₂(CH₂=CH₂)³⁰ were prepared according to reported procedures. NiCl₂dme (dme = 1,2-dimethoxyethane) and AgOTf (OTf = trifluoromethanesulfonate) were obtained from Strem Chemicals. Cl₂PPh₃, prepared by treatment of PPh₃ with PhICl₂, displayed spectral features identical to those reported in the literature.³¹ NiCl₂(PPh₃)₂ (1), Ni(PPh₃)₄ (5), tetrabutylammonium chloride (ⁿBu₄NCl), tetraethylammonium chloride (ⁿEt₄NCl), and triphenylphosphine (PPh₃) were obtained from Sigma Aldrich. All chemicals were used without further purification. Elemental analysis was obtained by Complete Analysis Laboratories, Inc., New Jersey. Evolved hydrogen was quantified by gas chromatography using a calibration curve derived from adding HCl to known quantities of NaH; over the relevant concentration range, the gas chromatograph response was linear. This procedure has previously been validated by comparison with Toepler pump combustion analysis.¹⁵

Preparation of Ni(II) trihalide complexes

Complex 2[CIPPh₃]. A solution of PhICl₂ (9.1 mg, 3.30 × 10⁻⁵ mol, 1.00 equiv.) in 1 mL of CH₂Cl₂ was added to a solution of NiCl₂(PPh₃)₂ (21.4 mg, 3.30 × 10⁻⁵ mol, 1.00 equiv.) in 2 mL of CH₂Cl₂ to prompt an immediate colour change from a light beige to blue. The solvent was removed *in vacuo*, and the resulting solid was treated with pentane. The pentane was decanted, and the resulting solid was dried *in vacuo* to afford 21.5 mg of title compound (90% yield). ¹H NMR (600 MHz, CD₃CN) δ (ppm): 7.77 (m, 9H), 7.64 (m, 6H). μ_{eff}(CH₃CN) = 4.20 μ_B. Anal. calcd (found) for C₃₆H₃₀Cl₄NiP₂: C, 59.63 (59.53); H, 4.17 (4.09). Crystals suitable for single-crystal diffraction analysis were obtained from a CH₃CN solution of the complex layered with Et₂O.

Complex 2[TBA]. To a suspension of NiCl₂(dme) (40.0 mg, 1.82 × 10⁻⁴ mol, 1.00 equiv.) in CH₂Cl₂ was added PPh₃ (47.7 mg, 1.82 × 10⁻⁴ mol, 1.00 equiv.) and ⁿBu₄NCl (50.6 mg, 1.82 × 10⁻⁴ mol, 1.00 equiv.) as a solid. The reaction solution immediately turned from yellow to blue. The reaction mixture was stirred at 23 °C for 1 h. The reaction was concentrated to dryness and the residue was taken up in pentane and Et₂O, solvent was decanted, and the residue was dried *in vacuo* to afford 119 mg of the title complex as a blue solid (98% yield). ¹H NMR (600 MHz, CD₃CN) δ (ppm): 3.32 (q, 2H), 1.83 (m, 2H), 1.53 (m, 2H), 1.08 (t, 3H). μ_{eff}(CH₃CN) = 4.02 μ_B. Anal. calcd (found) for C₃₄H₅₁Cl₃NNiP: C, 60.97 (60.93); H, 7.68 (7.58); N,

2.09 (2.06). Complex 2[TEA] was prepared analogously by substitution of ⁿBu₄NCl with ⁿEt₄NCl in 95% yield; ¹H NMR (600 MHz, CD₃CN) δ (ppm): 3.48 (q, 2H), 1.45 (t, 3H). μ_{eff}(CH₃CN) = 4.17 μ_B. Anal. calcd (found) for C₂₆H₃₅Cl₃NNiP: C, 56.01 (56.14); H, 6.33 (6.26); N, 2.51 (2.67). Crystals suitable for single-crystal diffraction analysis were obtained from a CH₃CN solution of the complex layered with Et₂O and unit cell data matched literature reports.³²

Preparation of [ClPPh₃]OTf

To a solution of Cl₂PPh₃ (127 mg, 3.81 × 10⁻⁴ mol, 1.00 equiv.) in CH₂Cl₂ was added AgOTf (98.0 mg, 3.81 × 10⁻⁴ mol, 1.00 equiv.) as a suspension in CH₂Cl₂. White solid immediately precipitated when AgOTf was added and the reaction mixture was stirred at 23 °C for 1 h before being filtered through Celite. The filtrate was concentrated *in vacuo* and the residue was taken up in THF and solvent was decanted, and the residue was dried *in vacuo* to afford 157 mg of the title compound as a white solid (92% yield). ³¹P NMR (160 MHz, CD₂Cl₂) δ (ppm): 66.4; ¹⁹F NMR (275 MHz, CD₂Cl₂) δ (ppm): -78.9. The spectral data is consistent with that reported for ClPPh₃·AlCl₄.³³ Crystals suitable for single-crystal diffraction analysis were obtained from a CH₂Cl₂ solution layered with Et₂O.

Preparation of Ni(II) tetrachloride complex [NiCl₄][Et₄N]

A solution of ⁿEt₄Cl (30.2 mg, 1.82 × 10⁻⁴ mol, 1.00 equiv.) in 2 mL of CH₂Cl₂ was added to a solution of NiCl₂(dme) (40.0 mg, 1.82 × 10⁻⁴ mol, 1.00 equiv.) in 2 mL of CH₂Cl₂ to prompt an immediate colour change from yellow to green. After stirring at 23 °C for 0.5 h, the reaction mixture was concentrated to dryness and the residue was taken up in pentane and solvent was decanted, and the residue was dried *in vacuo* to afford 77.2 mg of the title compound as a green solid (92% yield). Crystals suitable for single-crystal diffraction analysis were obtained from a CH₃CN solution layered with Et₂O and unit cell data matched literature reports.³⁴

Preparation of Ni(I) complexes

Complex 3. To a scintillation vial was added Ni(cod)₂ (58.0 mg, 2.10 × 10⁻⁴ mol, 1.00 equiv.) and NiCl₂(dme) (46.0 mg, 2.10 × 10⁻⁴ mol, 1.00 equiv.) as solids, followed by 3 mL of PhCH₃. To this solution was added PPh₃ (330 mg, 1.26 × 10⁻³ mol, 6.00 equiv.) dissolved in 2 mL PhCH₃ and the reaction mixture was stirred at 23 °C for 12 h before being filtered through Celite. The filtrate was concentrated *in vacuo* to a volume of 1.5 mL, layered with hexanes, and cooled to -30 °C to afford yellow crystalline solid (80% yield). ¹H NMR (600 MHz, THF-*d*₈) δ (ppm): 9.51 (br, s, 20H), 5.28 (br, s, 15H), 4.20 (br, s, 10H). μ_{eff}(CH₃CN) = 1.74 μ_B. Crystals suitable for single-crystal diffraction analysis were obtained from a PhCH₃ solution of the complex layered with *n*-hexane and collected unit cell data matched literature reports.³⁵

Complex 4. To a scintillation vial was added Ni(PPh₃)₂(CH₂=CH₂) (20.0 mg, 3.30 × 10⁻⁵ mol, 1.00 equiv.) and NiCl₂(PPh₃)₂ (21.4 mg, 3.30 × 10⁻⁵ mol, 1.00 equiv.) as solids followed by 4 mL of Et₂O. The reaction mixture was stirred at



23 °C for 0.5 h, during which time a yellow precipitate was observed. The mixture was concentrated to dryness and the residue was taken up in pentane and dried *in vacuo* to afford 18.4 mg of the title complex as a yellow solid (90% yield).³⁶

Results and discussion

We targeted phosphines as potential photoredox mediators for a tandem photoredox/transition metal catalysed H₂-evolution photocycle from HCl based on their demonstrated ability to serve as photochemical H-atom donors.²⁷ To evaluate the viability of the proposed phosphine-mediated photoredox approach for H₂ evolution, we photolyzed Ni(II) complex NiCl₂(PPh₃)₂ (**1**) in THF ($\lambda > 295$ nm) in the presence of 1.0 equiv. PPh₃ and 15 equiv. of HCl. The light beige reaction solution turned pale blue upon photolysis. Analysis of the headspace by gas chromatography (GC) confirmed H₂ as the exclusive gaseous product under these conditions; integration of the chromatogram and comparison to a H₂ calibration curve generated from the reaction of NaH with HCl revealed that 3.1 turnovers had been achieved in 18 h. NiCl₂(PPh₃)₂ participates in ligand dissociation equilibria to release PPh₃ (*vide infra*),³⁷ and thus H₂-evolving photocatalysis was also observed in the absence of exogenous PPh₃. Evaluation of the amount of H₂ evolved as a function of time (Fig. 1), showed that in the

presence of excess HCl, H₂ evolution continues and 9 turnovers were achieved after 44 h with no signs of deactivation.

During the photolysis of NiCl₂(PPh₃)₂, the blue-coloured solution that initially develops persists throughout subsequent H₂ evolution and based on UV-vis measurements, appears to represent the photoreacting state of the catalyst system. The pale blue photoproduct was identified as Ni(II) trihalide complex 2[ClPPh₃] by single-crystal X-ray diffraction analysis.[‡] In addition, comparison of the *in situ* UV-vis spectrum obtained during H₂-evolving catalysis with a spectrum obtained from an authentic sample of 2[ClPPh₃], prepared by treatment of NiCl₂(PPh₃)₂ with 1.0 equiv. of PhICl₂ (Fig. S15[†]), confirmed the identity of the catalyst resting state. Independently isolated complex 2[ClPPh₃] is chemically competent at H₂ generation under above photoreaction conditions.

Catalyst resting state 2[ClPPh₃] is constituted of a Ni trichloride anion and a phosphonium cation. In order to establish the roles of both the Ni complex and phosphine in the observed H₂ evolution reaction, 2[TBA] and phosphonium cation [ClPPh₃] OTf were independently prepared. As summarized in Table 1, Ni(II) complex 2[TBA] showed a similar activity toward HCl with 5.0 TON in 18 h. Complex 2[TBA] also participates in a minor equilibrium with free PPh₃ (*vide infra*) and thus both catalyst and photoredox mediator are present when 2[TBA] is employed as the photocatalyst. In contrast, phosphonium salt [ClPPh₃]OTf does not produce H₂ under the same reaction conditions. Additionally, neither PPh₃ or [NiCl₄][TEA]₂ is a competent H₂-evolution catalyst, confirming the necessity of both Ni complex and phosphine for productive H₂ evolution chemistry.

Fig. 2 illustrates a tandem catalytic cycle that accounts for the photogeneration of H₂ from HCl catalyzed by the Ni phosphine complexes and phosphine photoredox mediators. Diphenyl phosphine is initially formed by photochemical cleavage of the P–C bond and H-atom abstraction from solvent.²⁷ Photochemical cleavage of the P–H bond in HPPH₂ generates an H-atom equivalent and a diphenylphosphinyl radical.²⁷ The H-atom participates in halogen-atom abstraction with Ni(II) resting state **2** to generate a Ni(I) intermediate while the accompanying diphenylphosphinyl radical participates in C–H abstraction with solvent to regenerate the diphenylphosphine and close the photoredox cycle. Ni(I) intermediate **3** undergoes disproportionation to afford NiCl₂(PPh₃)₂ (**1**) and Ni(PPh₃)₄ (**5**). Protonolysis of Ni(0) complex **5** affords H₂ and regenerates Ni(II) dihalide **1**, thus closing the hydrogen

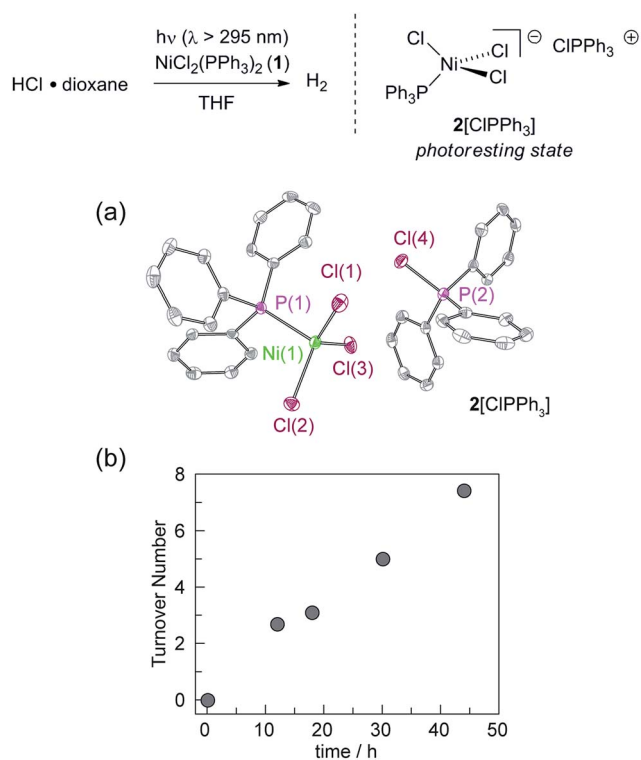


Fig. 1 Photolysis of NiCl₂(PPh₃)₂ in THF ($\lambda > 295$ nm) in the presence of 15 equiv. of HCl affords H₂ as well as 2[ClPPh₃]. (a) Thermal ellipsoid plot of 2[ClPPh₃] drawn at the 50% probability level. The hydrogen atoms are omitted for clarity. (b) Time-dependent turnover number (TON) of H₂ produced by a 4.5 mM THF solution of NiCl₂(PPh₃)₂ in the presence of 15 equiv. HCl ($\lambda > 295$ nm).

Table 1 TON of H₂ measured in the headspace upon photolysis of designated compounds in the presence of 15 equiv. HCl in THF for 18 h

| Compound | TON |
|--|-----|
| 2[ClPPh ₃] | 2.0 |
| PPh ₃ | 0 |
| [NiCl ₄][Et ₄ N] ₂ | 0 |
| 2[TBA] | 5.0 |
| [ClPPh ₃]OTf | 0 |



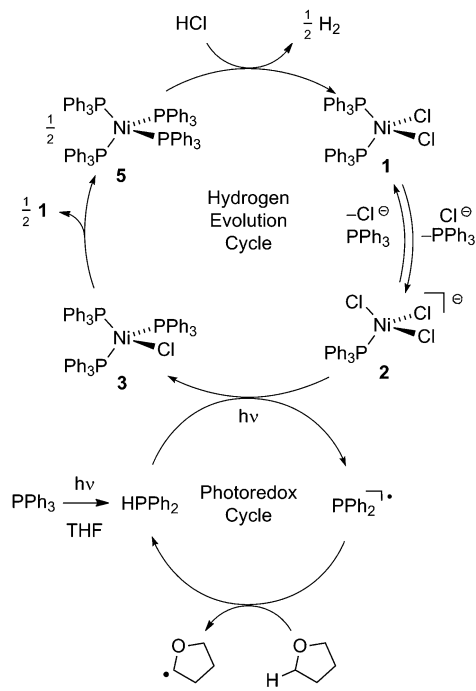


Fig. 2 Proposed tandem catalytic cycles for H₂-generation with Ni-based H₂-evolution catalysts and phosphine-based photoredox mediators.

evolution cycle. The number of phosphine ligands bound to intermediates in the tandem cycle illustrated in Fig. 2 is unknown. Isolated complexes 2[ClPPh₃], 3, 4 and 5, which display 1–4 phosphine ligands per Ni, are all competent catalysts for H₂ evolution and proceed with the same photoregulating state (2[ClPPh₃]), demonstrating ligand dissociation equilibria³⁷ are established during catalysis (Fig. S16†).

In order to probe the contention that photogenerated diphenylphosphinyl radicals could mediate the reduction of a Ni–Cl bond from the Ni(II) trihalide complex, we carried out time-resolved photochemical experiments. On the picosecond timescale, a transient absorption (TA) difference spectrum obtained by laser flash photolysis ($\lambda_{\text{exc}} = 310$ nm, THF solutions) of 2[TBA] exhibits a spectral growth centred at 506 nm with a lifetime of ~ 700 ps (Fig. S18†). An identical spectral feature was observed during laser flash photolysis of PPh₃ solutions. This feature was assigned to be that of the singlet excited state of PPh₃, and the observation of this signal in the TA spectrum of 2[TBA] supports the presence of a minor equilibrium between 2[TBA] and free PPh₃.³⁸ Additional support for this ligand dissociation equilibrium is the observation that both 2[TBA] and PPh₃ both show an emission band centred at 500 nm with a 900 ps lifetime (Fig. S17†), which is well-matched to reported PPh₃ photophysics.³⁹ The similar emission lifetimes for both 2[TBA] and PPh₃ excludes dynamic quenching of the excited ¹PPh₃* species by the Ni complex and suggests that the relatively low steady-state emission intensity observed for 2[TBA] is due only to a low equilibrium concentration of PPh₃.

The photochemistry of 2 and PPh₃ were also examined at longer time scales by nanosecond flash photolysis (Fig. 3). Flash

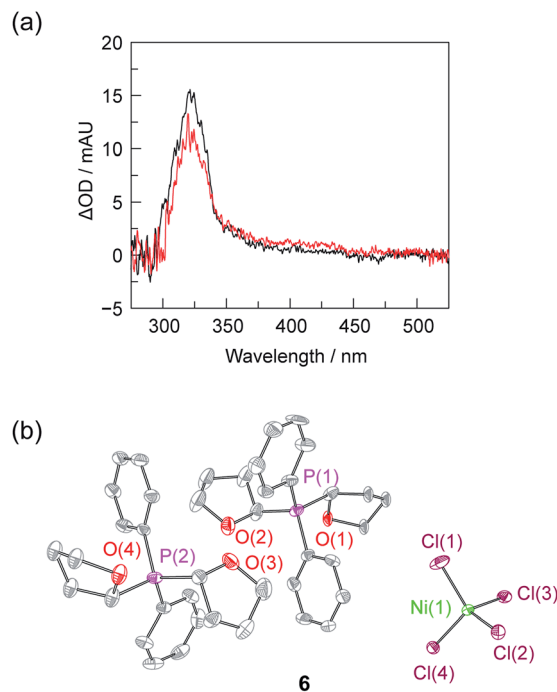
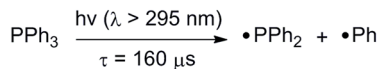


Fig. 3 (a) Nanosecond transient absorption (TA) spectroscopy of Ni complex 2[TEA] (—, red) and PPh₃ (—, black) is consistent with formation of diphenylphosphinyl radical. TA spectrum obtained by laser flash photolysis (310 nm pump) of a 1 : 1 THF : CH₃CN solution recorded at a 1 μs delay. (b) Thermal ellipsoid of 6 drawn at the 50% probability level. The hydrogen atoms are omitted for clarity.

photolysis of either 2[TEA] (red spectrum, Fig. 3) or PPh₃ (black spectrum, Fig. 3) leads to the observation of TA signals that are ascribed to diphenylphosphinyl radical.²⁷ The lifetime of the diphenylphosphinyl radical derived from PPh₃ with and without the presence of 2[TBA] in solution is the same, consistent with no direct reaction between Ni(II) complex and diphenylphosphinyl radical (Fig. S19†). Substantial phosphine consumption is not required for H₂ evolution because the diphenylphosphine generated during catalysis is a competent photoredox carrier. Nanosecond-resolved TA spectra, collected by laser flash photolysis of diphenylphosphine in THF, display the spectral features of diphenylphosphinyl radical (Fig. S20†), confirming that phosphine mediators can be catalytic.^{27,40}

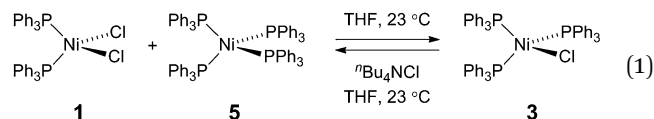
That the photogenerated diphenylphosphinyl radical engages in HAA with THF to produce diphenylphosphine is confirmed by the isolation of complex 6, as a photo-byproduct of the photolysis of Ni complex 2[TEA]. Complex 6 features two C-bound tetrahydrofuran ligands on a phosphorus centre and could be derived from reaction of photogenerated diphenylphosphinyl radicals with furanyl radicals derived from HAA chemistry. Additionally we observed (GC-MS) octahydro-2,2'-bifuran (homocoupled THF) as a photochemical byproduct. While HAA from THF by diphenylphosphinyl radicals is endothermic (16 kcal mol⁻¹ uphill based on P–H and C–H bond



dissociation energies),⁴¹ irreversible subsequent reactions, such as radical coupling to afford homocoupled THF sequester reactive radical intermediates.⁴⁰

The rate for HAA from solvent by photogenerated diphenylphosphinyl is strongly correlated with solvent C–H bond energies.^{27,42} We therefore anticipated that efficiency of the total catalytic process would be dictated by the turnover frequency of the photoredox mediator, which depends on the C–H BDEs of H-atom donor. The turnover frequency (TOF) of hydrogen generation from HCl with Ni complex 2 strongly depends on the solvent we employed, showing a positive correlation to the BDE of solvents: 0.34 h⁻¹ TOF in THF, 0.05 h⁻¹ TOF in CH₃CN, and 0.02 h⁻¹ TOF in C₆H₆ (92, 96, and 112 kcal mol⁻¹ of C–H BDEs respectively) (see Fig. S21† for details).^{43–45}

To probe the potential fate of potential Ni(I) intermediates during catalysis, we examined the chemistry of isolated Ni(I) complexes. Ni(I) complex 3 can be isolated from the comproportionation reaction of NiCl₂(PPh)₂ with Ni(PPh₃)₄. Based on the E°(Ni^{II}/Ni^I) and E°(Ni^I/Ni⁰) measured by cyclic voltammetry in THF (Fig. S22†), comproportionation is thermodynamically favored. In contrast, in the presence of exogenous chloride ion, added as tetrabutylammonium chloride, disproportionation of Ni(I) complex 3 to Ni(II) complex 1 and Ni(0) complex 5 is observed, as determined by both ³¹P NMR and electronic absorption spectroscopy (Fig. S8 and S14,† respectively). During H₂ evolution photocatalysis, chloride is present in large excess (68 mM) with respect to potential Ni(I) intermediates.



To assess whether the initially produced Ni(I) complex (3) or the Ni(0) complex (5) generated by disproportionation are active for H₂ production, we examined the stoichiometric H₂-evolution reaction chemistry of Ni(I) and Ni(0) complexes with HCl. The results of these experiments are summarized in Fig. 4. Treatment of Ni complexes 3, 4, and 5 with 15 equiv. HCl in THF generates H₂ in 44, 33, and 89% yields, respectively, along with Ni(II) complex 1, NiCl₂(PPh₃)₂. To gain insight into whether H₂ evolution proceeds by protonation of Ni(I) or Ni(0), generated by disproportionation reactions, electrochemical H₂ evolution was examined using Ni(II) trihalide complex 2[TEA]. As illustrated in Fig. 4, Ni complex 2[TEA] exhibits two electrochemically irreversible waves for the Ni^{II/I} and Ni^{I/0} couples at -1.62 and -1.95 V vs. Fc⁺/Fc, respectively. In the presence of excess HCl (pK_a = 8.9 in CH₃CN)⁴⁶ these two peaks exhibit catalytic cathodic waves. The dominant CV features of the Ni^{I/0} wave in the presence of excess HCl are consistent with Ni⁰ being involved in the H₂ generating steps in our photocatalysis.

Conclusions

As is common for first-row transition metal complexes, nickel halide complexes typically exhibit very short excited state lifetimes. Direct photoactivation of M–X bonds using the molecular excited states of these complexes has proven challenging owing to their short lifetimes. To circumvent the limitations imposed by short excited state lifetimes, we have developed a tandem photoredox/transition metal catalysis approach to H₂ evolution in which the chromophore and the H₂-evolution catalyst are localized on different molecules. Using diaryl phosphines as photoredox mediators, we have demonstrated that relatively non-basic phosphines are capable of acting as photoredox mediators under acidic conditions. Robust photocatalytic systems have been developed by combining phosphine photoredox mediators and Ni phosphine H₂-evolution catalysts. Time-resolved spectroscopy has revealed that phosphines serve as photochemical H-atom donors and activate the M–X bonds of Ni(II) halide complexes *via* halogen-atom abstraction. The H₂-evolution catalytic cycle is closed by sequential disproportionation of Ni(I) to afford Ni(0) and Ni(II) and protolytic H₂ evolution from the Ni(0) intermediate. The described photoredox strategy is attractive in that independent optimization of photoredox mediator and H₂-evolution catalyst provides multiple handles for system optimization.

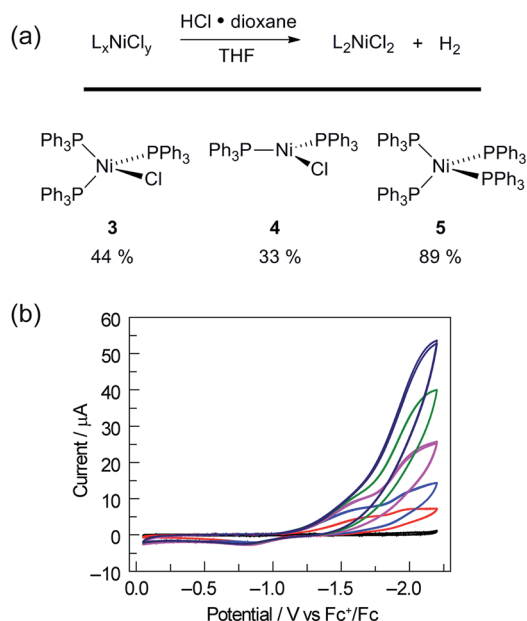


Fig. 4 (a) Protonation of Ni(I) and Ni(0) complexes afforded Ni(II) chloride as well as H₂. (b) Electrochemical response of electrolyte background (—, black), 1 mM Ni complex 2[TEA] (—, red) to addition of HCl 1.0 equiv. (—, blue), 5.0 equiv. (—, pink), 9.0 equiv. (—, green), 13.0 equiv. (—, dark blue) in CH₃CN (0.1 M NBu₄PF₆; scan rate, 100 mV s⁻¹). Glassy carbon working electrode, Ag/AgNO₃ reference, and Pt wire counter electrode.

Acknowledgements

We gratefully acknowledge Robert L. Halbach and D. Kwabena Bediako for helpful discussions, and the funding from NSF Grant CHE-1332783 and a Ruth L. Kirchenstein National Research Service award (F32GM103211) for D.C.P.



Notes and references

‡ Crystallographic data for 2[ClPPH₃]: C₃₆H₃₀Cl₄P₂Ni, *M* = 725.05, orthorhombic, *Pbca*, *a* = 17.435(4), *b* = 15.662(3), *c* = 24.139(9), *V* = 6591(2), *Z* = 8, μ = 1.036 mm⁻¹, *T* = 100(2) K, *R*₁ = 0.0527, *wR*₂ = 0.0720 (based on all reflections), *GooF* = 1.030, reflections measured = 57 380, unique reflections = 5858, *R*_{int} = 0.0741. Crystallographic data for 6: C₄₀H₄₈Cl₄O₄P₂Ni, *M* = 855.23, monoclinic, *P2₁/n*, *a* = 10.1261(8), *b* = 23.4579(18), *c* = 17.8192(14), β = 106.3550(12)°, *V* = 4061.4(5), *Z* = 4, μ = 0.859 mm⁻¹, *T* = 100(2) K, *R*₁ = 0.0788, *wR*₂ = 0.1328 (based on all reflections), *GooF* = 1.005, reflections measured = 44 051, unique reflections = 7212, *R*_{int} = 0.0668. Crystallographic data for Cl₂PPH₃: C₁₈H₁₅Cl₂P, *M* = 333.17, monoclinic, *P2₁/c*, *a* = 13.338(3), *b* = 14.376(3), *c* = 8.7454(17), β = 102.53(3)°, *V* = 1637.0(6), *Z* = 4, μ = 0.484 mm⁻¹, *T* = 100(2) K, *R*₁ = 0.0330, *wR*₂ = 0.0710 (based on all reflections), *GooF* = 1.060, reflections measured = 18 333, unique reflections = 2874, *R*_{int} = 0.0308. Crystallographic data for [ClPPH₃]OTf: C₁₉H₁₅ClF₃O₃PS, *M* = 446.79, monoclinic, *P2₁/n*, *a* = 11.255(2), *b* = 9.1501(18), *c* = 18.658(4), β = 93.04(3)°, *V* = 1918.7(7), *Z* = 4, μ = 0.438 mm⁻¹, *T* = 100(2) K, *R*₁ = 0.0425, *wR*₂ = 0.0737 (based on all reflections), *GooF* = 1.031, reflections measured = 18 058, unique reflections = 3392, *R*_{int} = 0.0362.

- 1 A. J. Esswein and D. G. Nocera, *Chem. Rev.*, 2007, **107**, 4022.
- 2 D. G. Nocera, *Inorg. Chem.*, 2009, **48**, 10001.
- 3 A. F. Heyduk and D. G. Nocera, *Science*, 2001, **293**, 1639.
- 4 A. J. Esswein, A. S. Veige and D. G. Nocera, *J. Am. Chem. Soc.*, 2005, **127**, 16641.
- 5 N. Elgrishi, T. S. Teets, M. B. Chambers and D. G. Nocera, *Chem. Commun.*, 2012, **48**, 9474.
- 6 T. R. Cook, Y. Surendranath and D. G. Nocera, *J. Am. Chem. Soc.*, 2009, **131**, 28.
- 7 T. S. Teets and D. G. Nocera, *J. Am. Chem. Soc.*, 2009, **131**, 7411.
- 8 T.-P. Lin and F. P. Gabbaï, *J. Am. Chem. Soc.*, 2012, **134**, 12230.
- 9 H. Yang and F. P. Gabbaï, *J. Am. Chem. Soc.*, 2014, **136**, 10866.
- 10 W. E. Van Zyl, J. M. López-de-Luzuriaga, J. P. Fackler Jr and R. J. Staples, *Can. J. Chem.*, 2001, **79**, 896.
- 11 J. P. Fackler Jr, *Inorg. Chem.*, 2002, **41**, 6959.
- 12 J. S. Ovens and D. B. Leznoff, *Dalton Trans.*, 2011, **40**, 4140.
- 13 T. A. Perera, M. Masjedi and P. R. Sharp, *Inorg. Chem.*, 2014, **53**, 7608.
- 14 A. R. Karikachery, H. B. Lee, M. Masjedi, A. Ross, M. A. Moody, X. Cai, M. Chui, C. D. Hoff and P. R. Sharp, *Inorg. Chem.*, 2013, **52**, 4113.
- 15 D. C. Powers, M. B. Chambers, T. S. Teets, N. Elgrishi, B. L. Anderson and D. G. Nocera, *Chem. Sci.*, 2013, **4**, 2880.
- 16 E. I. Carrera, T. M. McCormick, M. J. Kapp, A. J. Lough and D. S. Seferos, *Inorg. Chem.*, 2013, **52**, 13779.
- 17 For a recent counter-example, see: D. C. Powers, S. J. Hwang, S.-L. Zheng and D. G. Nocera, *Inorg. Chem.*, 2014, **53**, 9122.
- 18 C. H. Lee, D. A. Lutterman and D. G. Nocera, *Dalton Trans.*, 2013, **42**, 2355.
- 19 S. J. Tereniak, E. E. Marlier and C. C. Lu, *Dalton Trans.*, 2012, **41**, 7862.
- 20 E. A. Juban, A. L. Smeigh, J. E. Monat and J. K. McCusker, *Coord. Chem. Rev.*, 2010, **254**, 2677.
- 21 C. Creutz, M. Chou, T. L. Netzel, M. Okumura and N. Sutin, *J. Am. Chem. Soc.*, 1980, **102**, 1309.
- 22 C. H. Lee, T. R. Cook and D. G. Nocera, *Inorg. Chem.*, 2011, **50**, 714.
- 23 D. C. Powers, B. L. Anderson and D. G. Nocera, *J. Am. Chem. Soc.*, 2013, **135**, 18876.
- 24 K. Haav, J. Saame, A. Kütt and I. Leito, *Eur. J. Org. Chem.*, 2012, 2167.
- 25 Y. Sakaguchi and H. Hayashi, *J. Phys. Chem. A*, 2004, **108**, 3421.
- 26 D.-L. Versace, J. C. Bastida, C. Lorenzini, C. Cachet-Vivier, E. Renard, V. Langlois, J.-P. Malval, J.-P. Fouassier and J. Lalevée, *Macromolecules*, 2013, **46**, 8808.
- 27 S. K. Wong, W. Sytnyk and J. K. S. Wan, *Can. J. Chem.*, 1971, **49**, 994.
- 28 A. B. Pangborn, M. A. Giardello, R. H. Grubbs, R. K. Rosen and F. J. Timmers, *Organometallics*, 1996, **15**, 1518.
- 29 X.-F. Zhao and C. Zhang, *Synthesis*, 2007, **4**, 551.
- 30 K. D. Schramm and J. A. Ibers, *Inorg. Chem.*, 1980, **19**, 2441.
- 31 T. Yano, M. Hoshino, M. Kuroboshi and H. Tanaka, *Synlett*, 2010, **5**, 801.
- 32 M. C. Smith, S. C. Davies, D. L. Hughes and D. J. Evans, *Acta Crystallogr., Sect. E: Struct. Rep. Online*, 2001, **57**, m509.
- 33 A. Schmidpeter and S. Lochschmidt, *Inorg. Synth.*, 1990, **27**, 253.
- 34 G. D. Stucky, J. B. Folkers and T. J. Kistenmacher, *Acta Crystallogr.*, 1967, **23**, 1064.
- 35 D. D. Ellis and A. L. Spek, *Acta Crystallogr., Sect. C: Cryst. Struct. Commun.*, 2000, **56**, 1067.
- 36 N. C. Norman, A. G. Orpen, M. J. Quayle and G. R. Whittell, *Acta Crystallogr., Sect. C: Cryst. Struct. Commun.*, 2002, **58**, m160.
- 37 G. Bontempelli, F. Magno, M. D. Nobili and G. Schiavon, *J. Chem. Soc., Dalton Trans.*, 1980, 2288.
- 38 Y. Sakaguchi and H. Hayashi, *Chem. Phys. Lett.*, 1995, **245**, 591.
- 39 L. Maini, D. Braga, P. P. Mazzeo and B. Ventura, *Dalton Trans.*, 2012, **41**, 531.
- 40 M. L. Kaufman and C. L. Griffin, *Tetrahedron Lett.*, 1965, **12**, 769.
- 41 R. Waterman, *Curr. Org. Chem.*, 2008, **12**, 1322.
- 42 J. P. Roth, S. Lovell and J. M. Mayer, *J. Am. Chem. Soc.*, 2000, **122**, 5486.
- 43 L. J. J. Laarhoven, P. Mulder and D. D. M. Wayner, *Acc. Chem. Res.*, 1999, **32**, 342.
- 44 A. Cherkasov and M. Jonsson, *J. Chem. Inf. Comput. Sci.*, 2000, **40**, 1222.
- 45 W. van Scheppingen, E. Dorrestijn, I. Arends and P. Mulder, *J. Phys. Chem. A*, 1997, **101**, 5404.
- 46 V. Fourmond, P.-A. Jacques, M. Fontecave and V. Artero, *Inorg. Chem.*, 2010, **49**, 10338.

